NACA RM L56I20

NACA

RESEARCH MEMORANDUM

LIMITED INVESTIGATION OF EFFECTS OF DIFFERENTIAL HORIZONTAL-TAIL DEFLECTION ON LATERAL CONTROL CHARACTERISTICS OF TWO SWEPT-WING AIRPLANE MODELS AT MACH NUMBERS FROM 1.4 TO 2.0

By M. Leroy Spearman

Langley Aeronautical Laboratory
Langley Field, Va.

NATIONAL ADVISORY COMMITTEE FOR AERONAUTICS

WASHINGTON

December 13, 1956
Declassified May 29, 1961

NACA RM L56I20

NATIONAL ADVISORY COMMITTEE FOR AERONAUTICS

RESEARCH MEMORANDUM

LIMITED INVESTIGATION OF EFFECTS OF DIFFERENTIAL HORIZONTAL-TAIL DEFLECTION ON LATERAL CONTROL CHARACTERISTICS OF TWO SWEPT-WING AIRPLANE MODELS AT MACH NUMBERS FROM 1.4 TO 2.0

By M. Leroy Spearman

SUMMARY

A limited investigation has been made in the Langley 4- by 4-foot supersonic pressure tunnel to determine the effectiveness of differential horizontal-tail deflection for producing lateral control for two swept-wing airplane models in the Mach number range from 1.4 to 2.0. The tests were limited to rather small tail deflections but included combined angles of attack and sideslip up to about 20°. One model had a wing and tail swept 35°, whereas the other had a wing and tail swept 45°.

The tests showed the rolling-moment effectiveness to be essentially constant with sideslip angle but to decrease with increasing angle of attack. Estimates of the rolling-moment effectiveness near zero angle of attack were in reasonably good agreement with the experimental values, although they were consistently higher by 10 to 15 percent. The yawing moment due to control deflection was generally favorable at low angles of attack, but it became adverse with increasing angle of attack. Differential deflections of the tail had no significant effect on the longitudinal stability characteristics.

INTRODUCTION

A problem of concern is that of providing satisfactory roll control for airplanes in supersonic flight. The deflection of conventional outboard wing trailing-edge ailerons may result in large amounts of wing twist that cause the rolling power to be substantially reduced or even reversed. The wing twist may be reduced by locating the ailerons farther inboard, but the deflected controls may then cause undesirable flow disturbances in the region of the tail. Wing spoilers may be used to provide

roll control without the danger of wing twist; however, the spoiler-type control generally has undesirable nonlinear characteristics; particularly for small rates of roll.

Another method that has been suggested as a means for providing roll control involves the use of a differentially deflected horizontal tail. Such a control, of course, would avoid the wing-twist problem, although problems of nonlinearities and more complicated tail structures may still be involved. A summary of results for this type of control at subsonic, transonic, and supersonic speeds up to a Mach number of 2 is presented in reference 1.

The present paper presents results that are more detailed on the effectiveness of the horizontal tail as a roll control device for two of the configurations included in reference 1. These results were obtained for a Mach number range from 1.4 to 2.0 in the Langley 4- by 4-foot supersonic pressure tunnel during some investigations that had other primary objectives. The results are limited to rather small deflections of the tail but do include angles of attack and sideslip up to about 20°. One model had a wing and tail swept 35°, and the other had a wing and tail swept 45°.

COEFFICIENTS AND SYMBOLS

The results are presented as coefficients of forces and moments on the stability axis system (fig. 1) with the reference centers of gravity at longitudinal stations corresponding to the quarter-chord point of the wing mean geometric chord. The symbols are defined as follows:

C_n yawing-moment coefficient, $\frac{M_Z}{qSb}$

C_l rolling-moment coefficient, $\frac{M_X}{qSb}$

C_Y lateral-force coefficient, $\frac{Y}{qS}$

C_L lift coefficient, where Lift = -Z, $\frac{\text{Lift}}{qS}$

C_X longitudinal-force coefficient (corresponds to negative drag coefficient at zero sideslip), $\frac{X}{qS}$

C_m	pitching-moment coefficient, $\frac{M_Y}{qS\bar{c}}$
X	force along X-axis
Y	force along Y-axis
Z	force along Z-axis
M_X	rolling moment
M_Y	pitching moment
M_Z	yawing moment
S	wing area
S_t	horizontal-tail area
b	wing span
$\bar{c}$	wing mean geometric chord
c	chord
q	free-stream dynamic pressure
y_t	lateral center-of-pressure location of one panel of horizontal tail
β	angle of sideslip, deg
α	angle of attack, deg
δ_t	all-movable horizontal-tail incidence angle (see fig. 1), deg
M	free-stream Mach number
L	left tail panel
R	right tail panel
C_{l_δ}	rolling-moment coefficient due to tail deflection, $\Delta C_l/\Delta\delta_t$
C_{n_δ}	yawing-moment coefficient due to tail deflection, $\Delta C_n/\Delta\delta_t$

$C_{L_{\alpha_t}}$ lift-curve slope of horizontal tail

$\Delta\delta_t$ total differential tail-deflection angle

MODELS AND APPARATUS

Three-view drawings of the models are presented in figure 2. The geometric characteristics of the models are presented in table I.

Model 1 (see fig. 2(a)) had a wing with 35° sweep of the quarter-chord line, an aspect ratio of 4, a taper ratio of 0.5, and NACA 65A-series airfoil sections having thickness ratios of 6 percent at the root and 4 percent at the tip. The wing was mounted in a semihigh position on the body and had a negative dihedral of 2.5° and an incidence of 0°. An all-movable horizontal tail swept back 35° was mounted slightly below the wing-root chord line extended. A total deflection angle of -10° was obtained by deflecting the right tail panel -5° (trailing edge up) and the left tail panel -5° (trailing edge down).

Model 2 (fig. 2(b)) had a wing with 45° sweep of the quarter-chord line, an aspect ratio of 4, a taper ratio of 0.2, and NACA 65A004 airfoil sections. The wing was mounted on the body center line and had dihedral and incidence of 0°. An all-movable horizontal tail swept back 45° was located in the extended chord plane of the wing. Total deflections of -12° and -6° were used with model 2. The total deflection of -12° was obtained by deflecting the right tail panel -6° and the left tail panel -6°. The total deflection of -6° was obtained by deflections of the right and left tail panels of either -3° and -3°, respectively, or of -6° and 0°, respectively.

Forces and moments were measured by the use of six-component strain-gage balances contained in the sting-mounted models. Two different balance and sting arrangements were used for the two models.

TESTS, CORRECTIONS, AND ACCURACY

The test conditions are summarized as follows:

Configuration	M	Stagnation temperature, °F	Stagnation pressure, lb/sq ft	Reynolds number, based on $\bar{c}$
Model 1	1.61 2.01	100 100	1,440 1,440	1.56×10^6 1.35
Model 2	1.41 2.01	110 110	1,440 1,730	1.68 1.84

The stagnation dewpoint was maintained sufficiently low (below -25° F) to prevent condensation effects in the test section. The angles of attack and sideslip were corrected for the deflection of the balance and sting under load. The base pressure was measured and the longitudinal force was adjusted to a base pressure equal to the free-stream static pressure.

The maximum estimated error in each of the individual measured quantities is as follows:

Quantity	Model 1	Model 2
C_n	±0.0002	±0.0005
C_l	±.0001	±.0004
C_Y	±.0015	±.0010
C_L	±.0070	±.0080
C_X	±.0020	±.0020
C_m	±.0005	±.0004
δ_t	±.1	±.2
α	±.2	±.2
β	±.2	±.2

An index of figures 3 to 11, including the test angle ranges, is presented in table II.

DISCUSSION

Rolling Moment

Effects of angle of attack and sideslip.- The rolling moments provided by differential tail deflection were essentially constant throughout the sideslip range for any angle of attack for model 1 at $M = 1.61$ and $M = 2.01$ (figs 3 and 4). Limited sideslip data obtained for model 2 at $M = 2.01$ (fig. 8) indicated a similar result. However, the rolling effectiveness C_{l_δ} for both models decreased with increasing angle of attack, and between $\alpha = 16°$ and $\alpha = 20°$ values of C_{l_δ} were about one-half those at low angles of attack (fig. 9).

The limiting angles of sideslip for which the 10° tail deflection of model 1 would be able to neutralize the rolling moment due to sideslip (fig. 11) vary from a maximum of about 6° at low angles of attack

to angles of only about 2° at $\alpha \approx 15^\circ$. These limiting angles of sideslip could be increased with increased tail deflection until the tail loses effectiveness. This measure of the utility of differential tail deflection as a roll control device is, of course, limited to configurations and Mach numbers similar to those tested, because these results depend not only on the lift effectiveness of the tail but on the effective dihedral of the configuration as well.

Estimated rolling-moment effectiveness.- Estimated values of C_{l_δ} for differential tail deflections at $\alpha = 0^\circ$ were obtained from the relation

$$C_{l_\delta} = \frac{1}{2} C_{L_{\alpha_t}} \frac{y_t S_t}{bS}$$

The lateral center-of-pressure location of the tail y_t was obtained through the use of reference 2. For the present models the lateral center of pressure was found to be at approximately 40 percent of the exposed semispan of the tail. The lift-curve slope for the exposed tail was obtained by the use of reference 3. This procedure neglects body-tail interference effects. The estimated values thus obtained are in reasonably good agreement with the experimental values at $\alpha = 0^\circ$ but are consistently higher than the experimental values by approximately 10 to 15 percent (fig. 9). Part of this difference may be attributed to some dynamic-pressure loss at the tail and some loss of lift on the tail resulting from the small gap at the inboard end of the tail panels. Unpublished results from other tests of model 1 have shown that the presence of the wing reduces the horizontal-tail pitching-moment effectiveness approximately 10 percent. A similar reduction might be expected in rolling-moment effectiveness.

Effects of vertical tail.- Tests made with model 2 at $M = 1.41$ with the vertical tail both on and off indicated no measurable difference in the rolling effectiveness for the small tail-deflection angles investigated (fig. 7). This result may not be true, however, for larger tail deflections or for other possible tail arrangements.

Effects of initial pitch-control deflections.- Limited tests made with model 2 at $M = 1.41$ with a differential tail deflection of -6° indicated no difference in the rolling effectiveness for an initial pitch-control deflection of -3° (0° left, -6° right) from that obtained with an initial pitch-control deflection of 0° (-3° left, -3° right) (fig. 7). This result may not necessarily apply for higher initial pitch-control deflections, however, since under some conditions the differential deflections may result in the angle of attack for one tail panel exceeding the linear range of the tail lift-curve slope.

Yawing Moment

At angles of attack near zero, the yawing moments due to differential tail deflection were favorable for model 1 and were approximately zero for model 2 (fig. 10). For model 1, the favorable yawing moments are apparently a result of an initial downward flow angle at the tail that, when the tail is deflected differentially to provide positive roll, would result in the local angle of the left tail panel approaching zero while the local angle of the right tail panel becomes more negative. Consequently, the drag increment provided by the right tail panel would increase and thus provide a positive or favorable yaw. The existence of this initial downward flow angle at the tail is indicated by the effective downwash-angle measurements presented in reference 4 for a configuration similar to model 1 at $M = 1.41$.

For model 2, no yawing moments should be expected at $\alpha = 0^\circ$ because the tail is located symmetrically with respect to the body and wing, and the initial flow angle at the tail should be 0°. Hence, the differential tail deflection would result in equal drag increments for the left and right panels and would cause no yaw. With increasing angle of attack, the yawing moments become adverse for both models.

The limited tests made for model 2 at $M = 1.41$ indicated no effect of the vertical tail or of initial pitch-control deflection on the yawing-moment characteristics (fig. 7). Some effect might be expected, however, for larger deflection angles since other investigations have indicated that large symmetrical deflections of a horizontal tail have a significant effect on the lateral-force contribution of the vertical tail.

Longitudinal Stability Characteristics

For the small range of control deflections investigated, there was no significant effect of differential tail deflection on the longitudinal stability characteristics of either model (figs. 5 to 8).

CONCLUSIONS

An investigation has been made in the Langley 4- by 4-foot supersonic pressure tunnel to determine the effects of small differential horizontal-tail deflections on the lateral control characteristics of two swept-wing airplane models in the Mach number range from 1.4 to 2.0. One model had a wing and tail swept 35°, whereas the other had a wing and tail swept 45°. The results of the tests indicated the following conclusions:

1. The rolling moment provided by differential tail deflection was essentially constant throughout the sideslip range but decreased with increasing angles of attack α to values between approximately $\alpha = 16^\circ$ and $\alpha = 20^\circ$ that were about one-half the values at low angles of attack.

2. Estimates of the rolling-moment effectiveness at low angles of attack were in reasonably good agreement with the experimental values, although the estimates were consistently higher by 10 to 15 percent.

3. The yawing moment due to control deflection varied from favorable to approximately zero at low angles of attack but became adverse with increasing angle of attack.

4. For the small range of control deflections investigated, there was no significant effect of differential tail deflection on the longitudinal stability characteristics.

Langley Aeronautical Laboratory,
National Advisory Committee for Aeronautics,
Langley Field, Va., August 31, 1956.

REFERENCES

1. Campbell, John P.: The Use of the Horizontal Tail for Roll Control. NACA RM L55L16a, 1956.

2. Sherman, Windsor L., and Margolis, Kenneth: Theoretical Calculations of the Effects of Finite Sideslip at Supersonic Speeds on the Span Loading and Rolling Moment for Families of Thin Sweptback Tapered Wings at an Angle of Attack. NACA TN 3046, 1953.

3. Harmon, Sidney M., and Jeffreys, Isabella: Theoretical Lift and Damping in Roll of Thin Wings With Arbitrary Sweep and Taper at Supersonic Speeds - Supersonic Leading and Trailing Edges. NACA TN 2114, 1950.

4. Palazzo, Edward B., and Spearman, M. Leroy: Static Longitudinal and Lateral Stability and Control Characteristics of a Model of a 35° Swept-Wing Airplane at a Mach Number of 1.41. NACA RM L54G08, 1955.

TABLE I.- GEOMETRIC CHARACTERISTICS OF MODELS

Characteristic	Model 1	Model 2
Wing		
Area, including body intercept, sq in.	160.21	144
Span, in.	25.31	24
Root chord, in.	8.44	10
Tip chord, in.	4.22	2
Mean geometric chord, in.	6.55	6.89
Sweep of quarter-chord line, deg	35	45
Aspect ratio	4	4
Taper ratio	0.5	0.2
Airfoil section	NACA 65A006 (root) NACA 65A004 (tip)	NACA 65A004
Horizontal tail		
Area, including body intercept, sq in.	41.9	28.7
Area, exposed, sq in.	28.2	18.24
Span, in.	12.12	10.73
Root chord, in.	4.94	3.35
Tip chord, in.	1.98	2.01
Sweep of quarter-chord line, deg	35	45
Aspect ratio (total)	3.5	4
Aspect ratio (exposed)	3	3
Taper ratio	0.4	0.6
Airfoil section	NACA 65A006 (root) NACA 65A004 (tip)	Hexagonal
Vertical tail		
Area, sq in.	25.6	42.3
Span, in.	6.2	8.59
Root chord, in.	7.0	8.18
Tip chord, in.	1.24	1.64
Sweep of quarter-chord line, deg	44.5	35
Aspect ratio	3	3.5
Taper ratio	0.177	0.2
Airfoil section	NACA 65A006 (root) NACA 65A004 (tip)	Hexagonal

TABLE II.- INDEX OF FIGURES 3 TO 11

Model	M	α, deg	β, deg	Component	Figure
Basic data					
1	1.61	0, 4.2, 8.5, 12.7, 16	Range	C_n, C_l, C_Y	3
1	2.01	0, 4.1, 8.3, 12.5, 15.5	Range	C_n, C_l, C_Y	4
1	1.61	Range	0	C_L, C_X, C_m C_n, C_l, C_Y	5
1	2.01	Range	0	C_L, C_X, C_m C_n, C_l, C_Y	6
2	1.41	Range	0	C_L, C_X, C_m C_n, C_l, C_Y	7
2	2.01	Range	0,4	C_L, C_X, C_m C_n, C_l, C_Y	8
Summary					
1,2	Various	C_{l_δ} against α			9
1,2	Various	C_{n_δ} against α			10
1	1.61, 2.01	β against α for trim roll			11

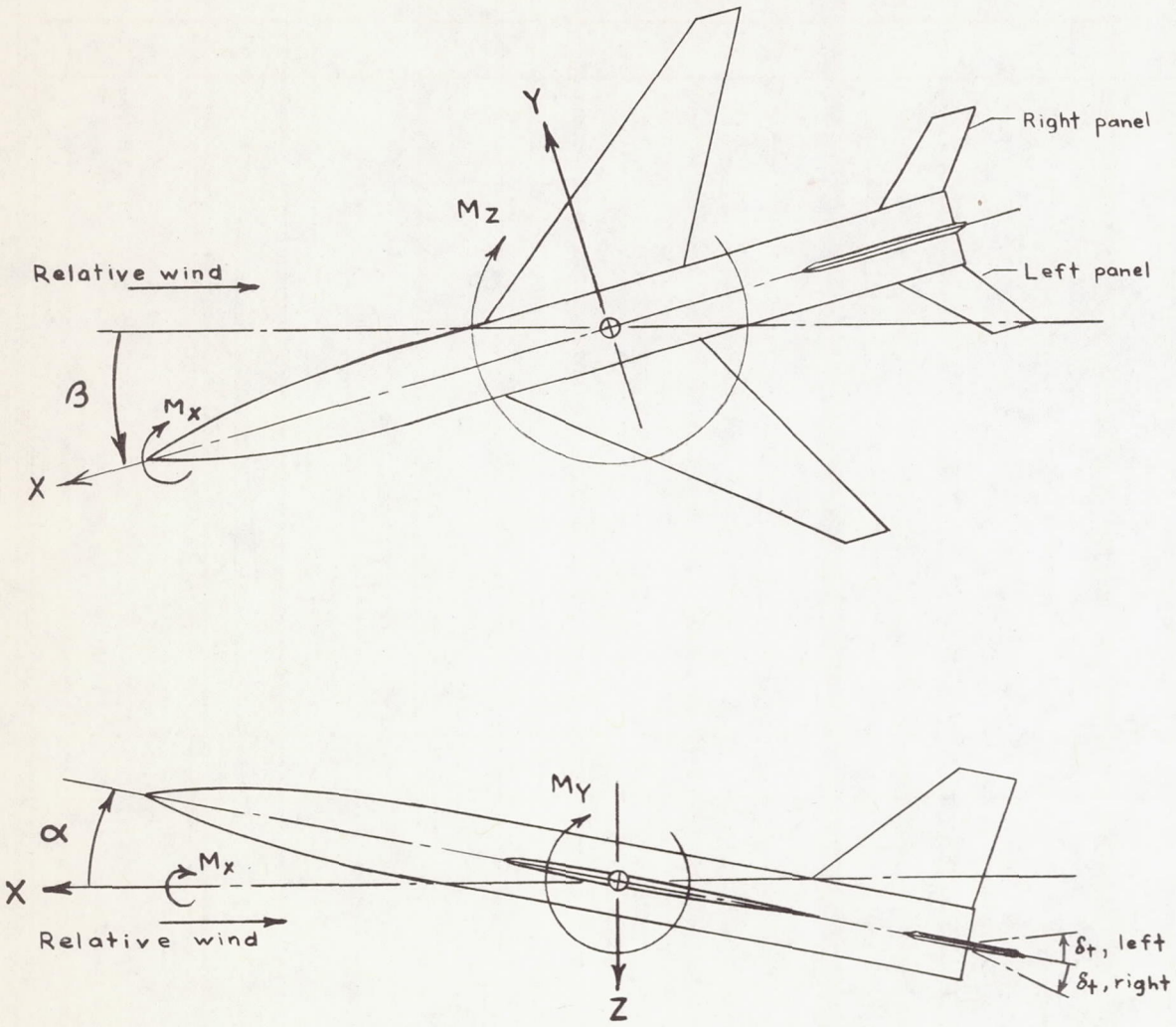
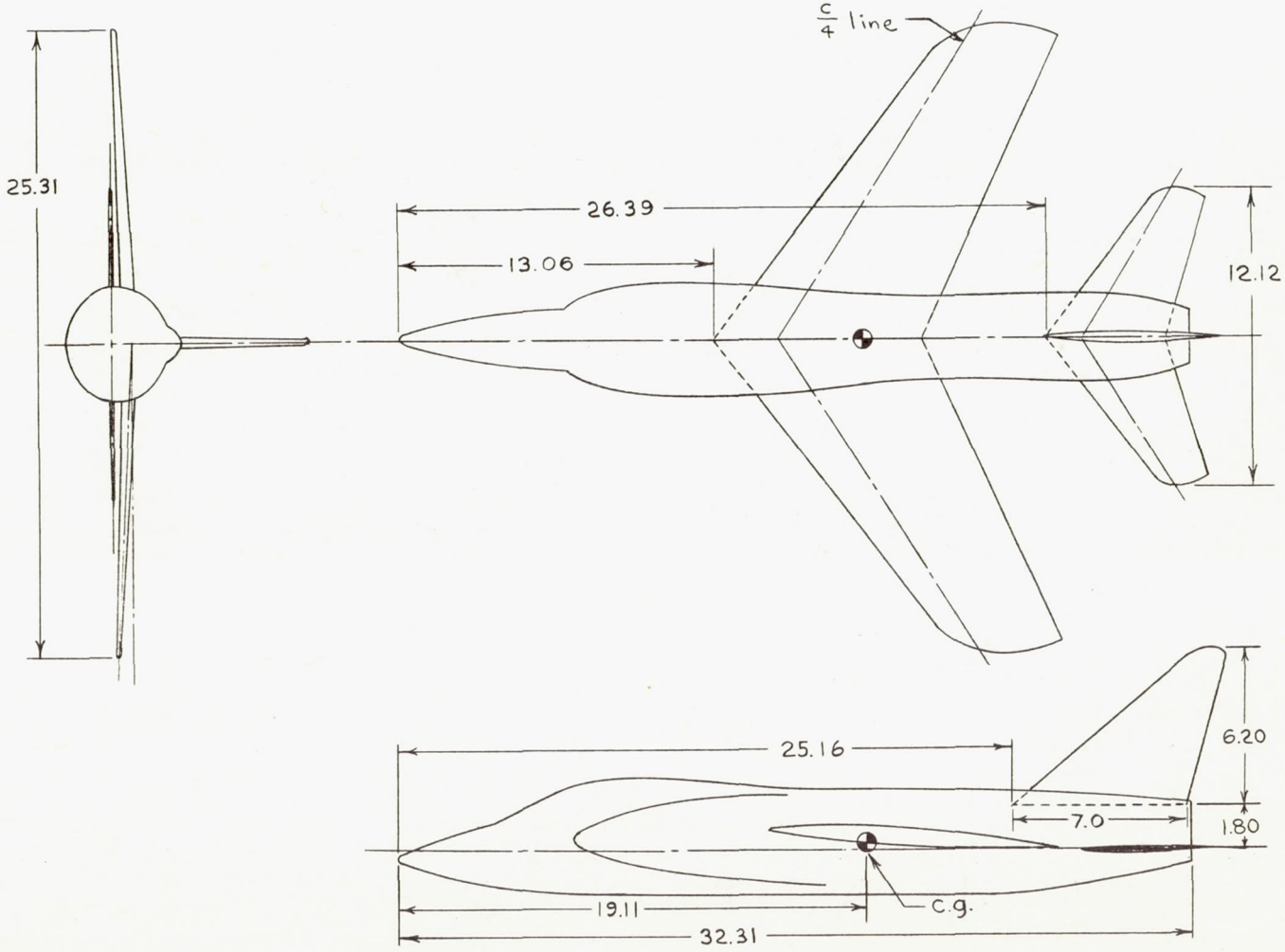
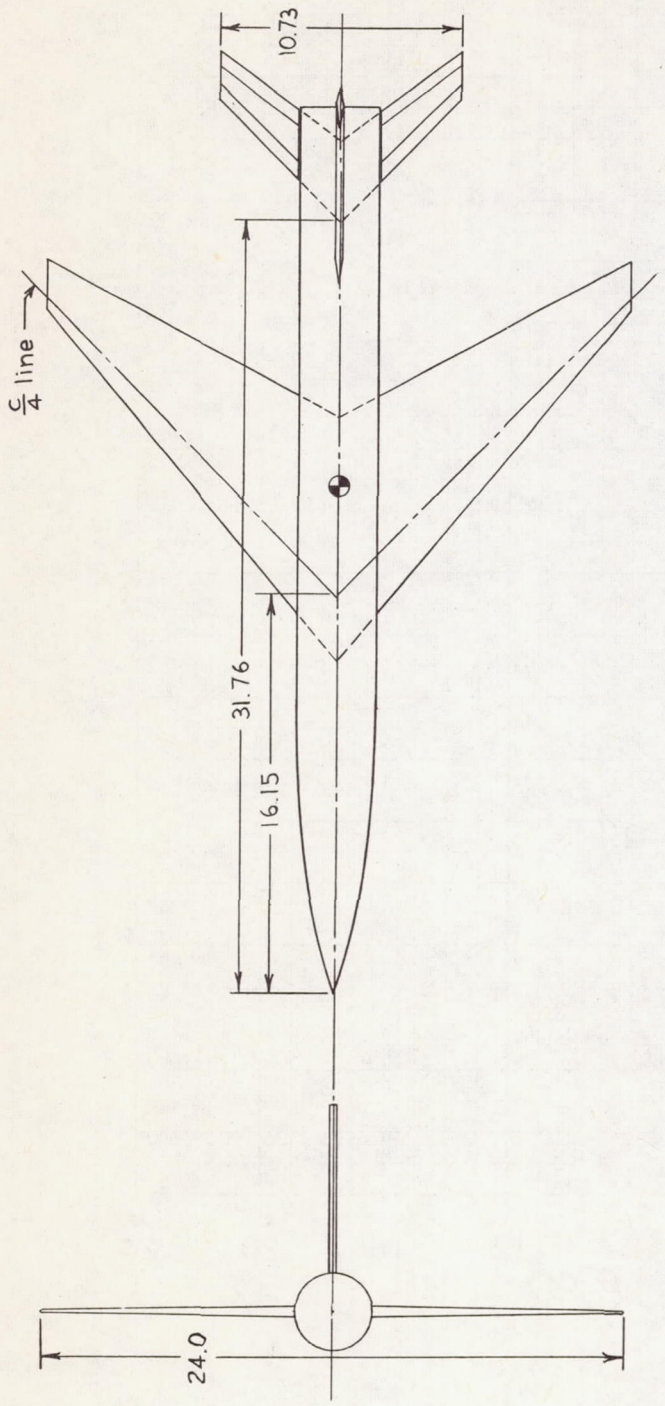


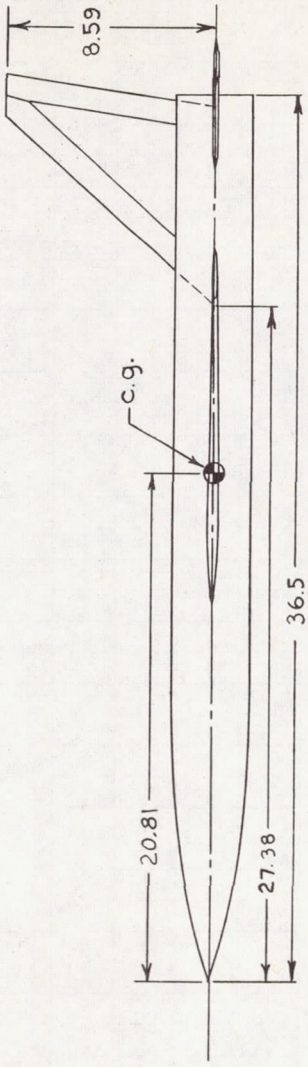
Figure 1.- System of stability axes. Arrows denote positive directions.



(a) Model 1.

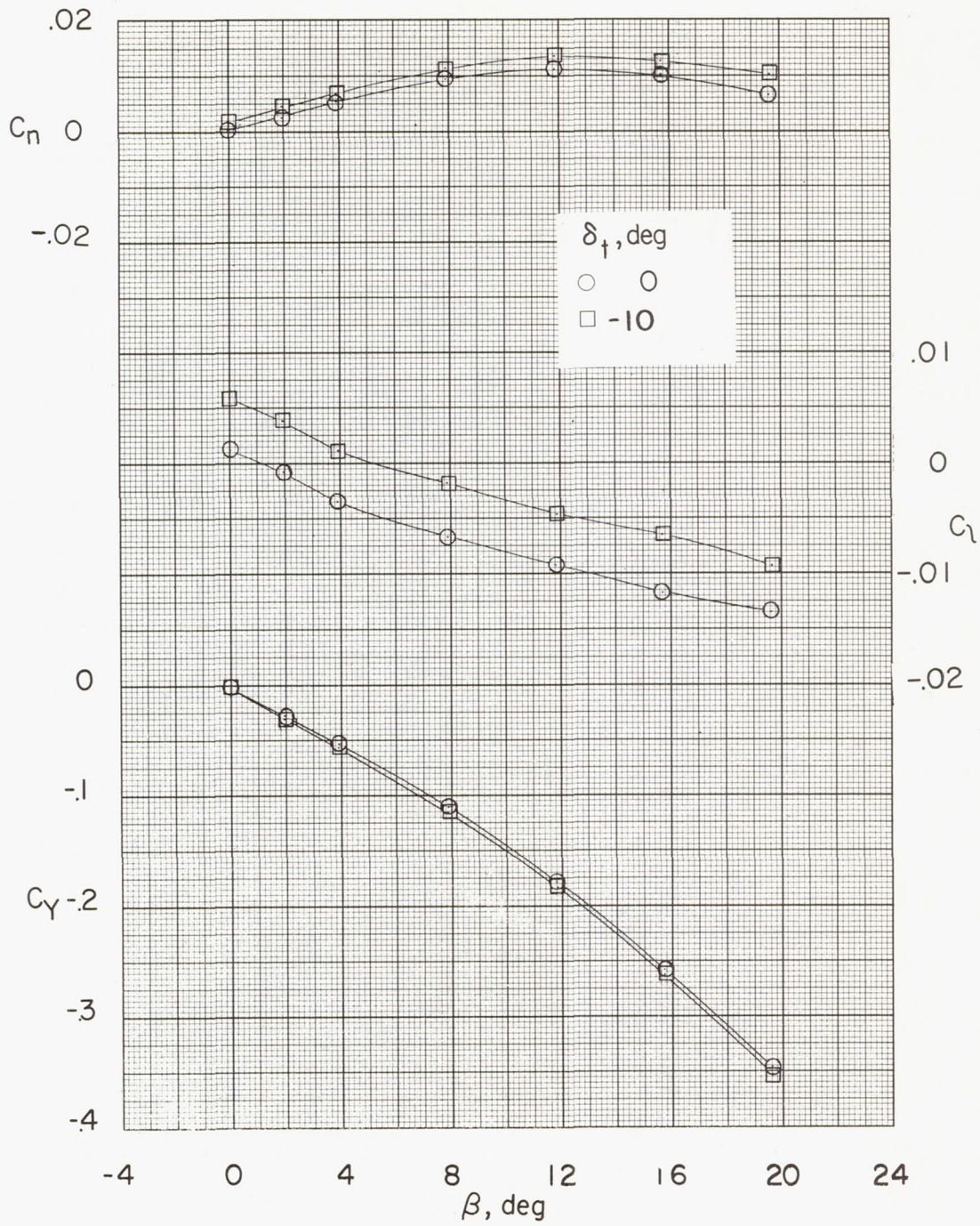
Figure 2.- Details of models.





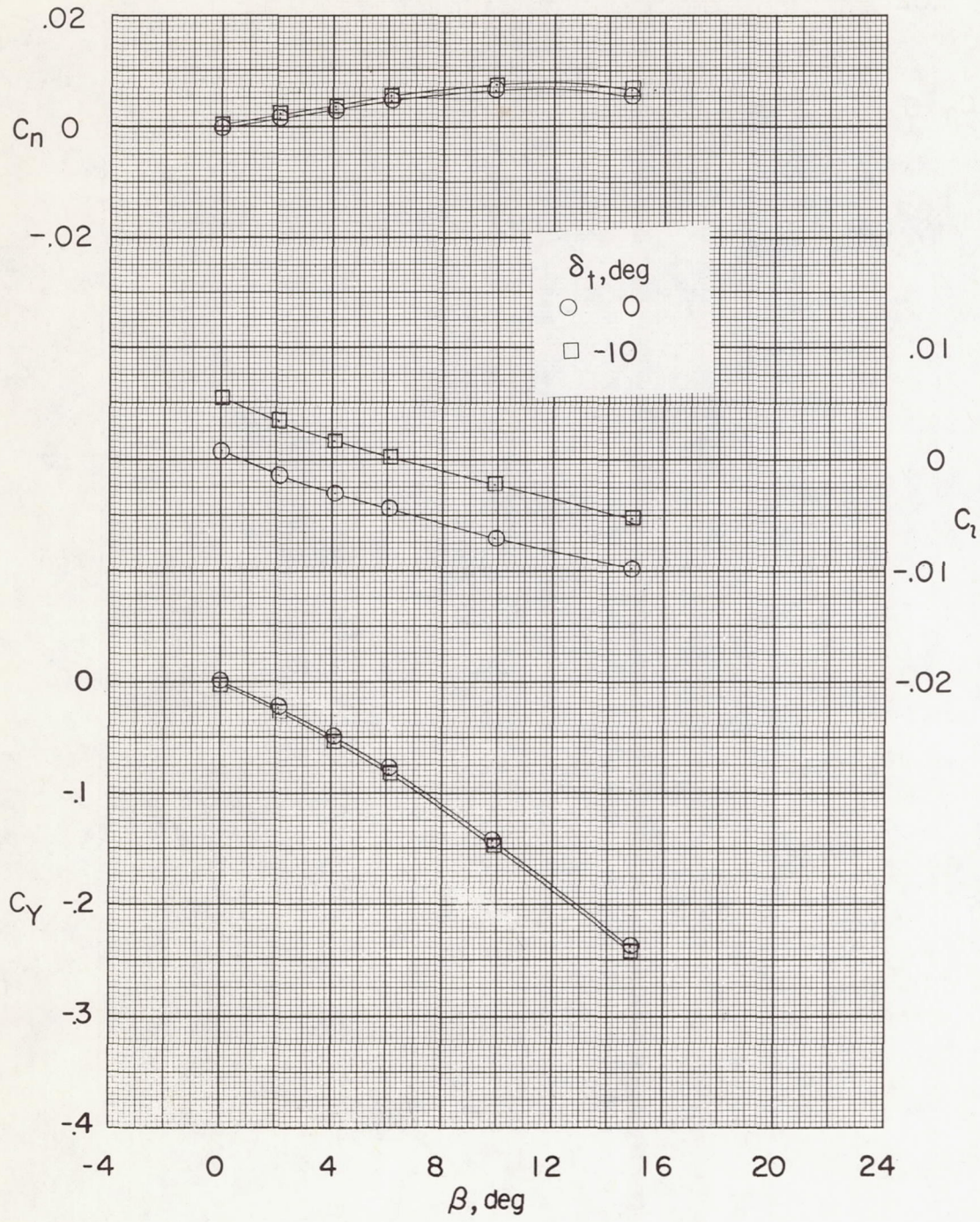
(b) Model 2.

Figure 2.- Concluded.



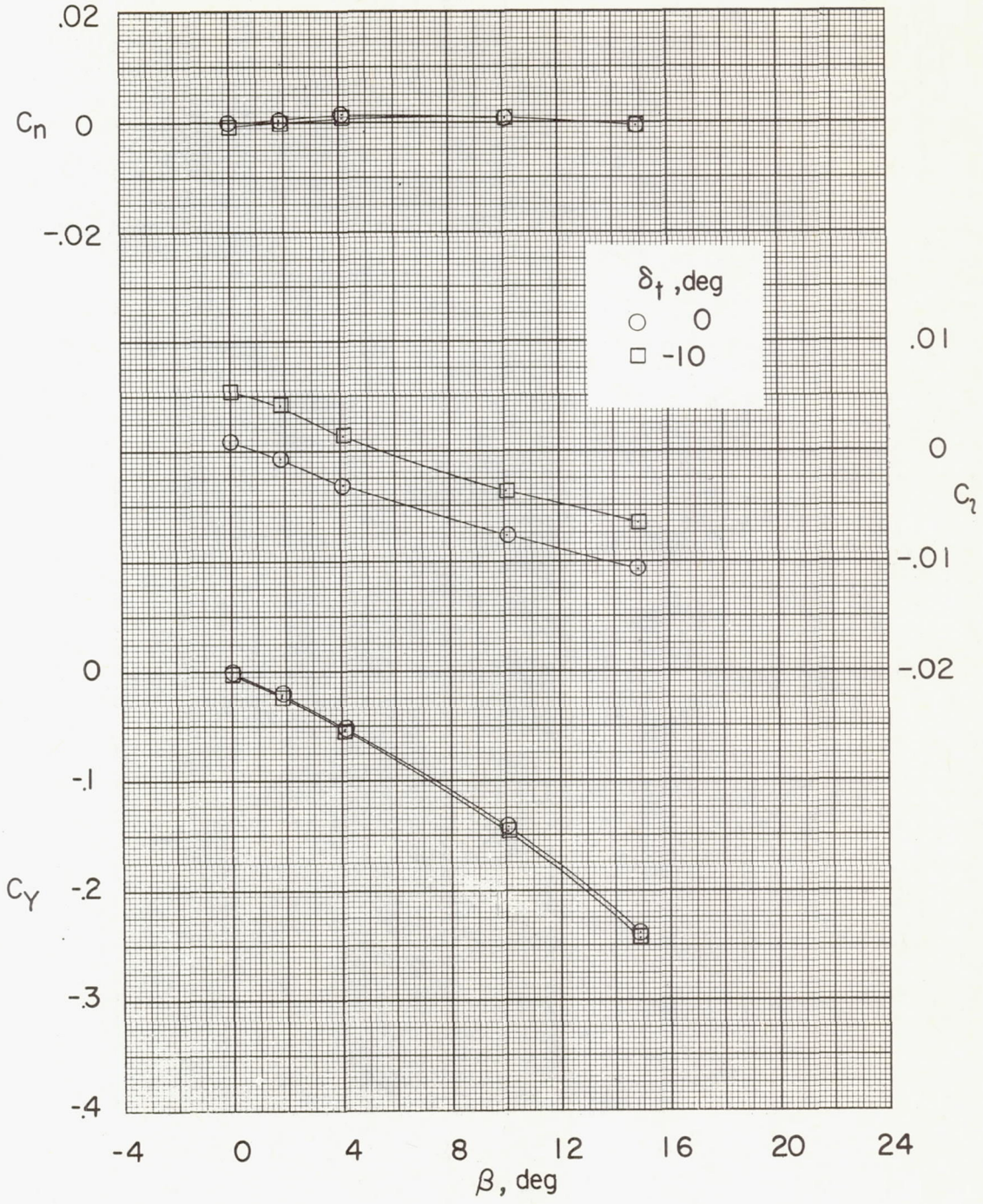
(a) $\alpha \approx 0^\circ$.

Figure 3.- Effect of differential stabilizer deflection on the aerodynamic characteristics in sideslip. Model 1; M = 1.61.



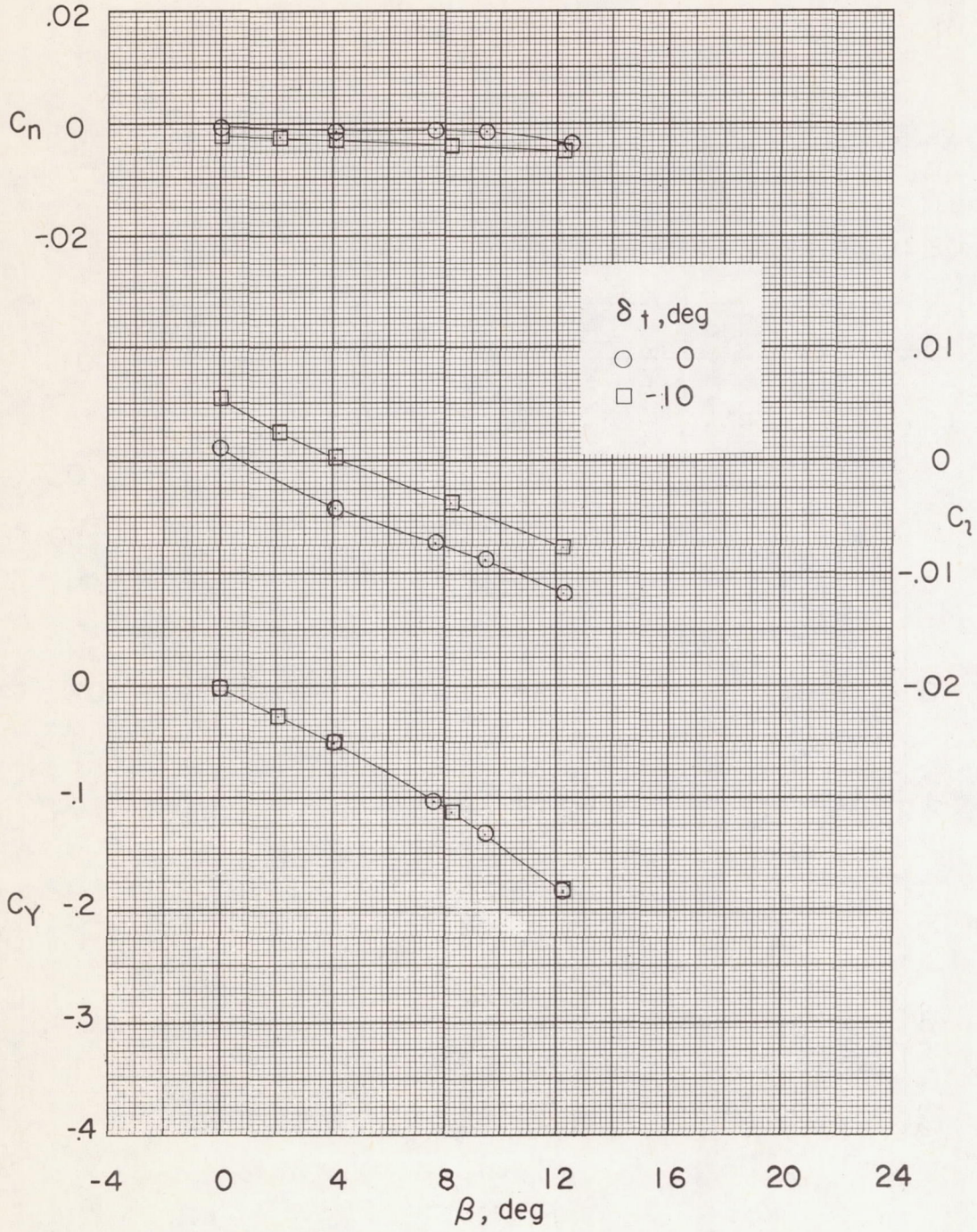
(b) $\alpha \approx 4.2^\circ$.

Figure 3.- Continued.



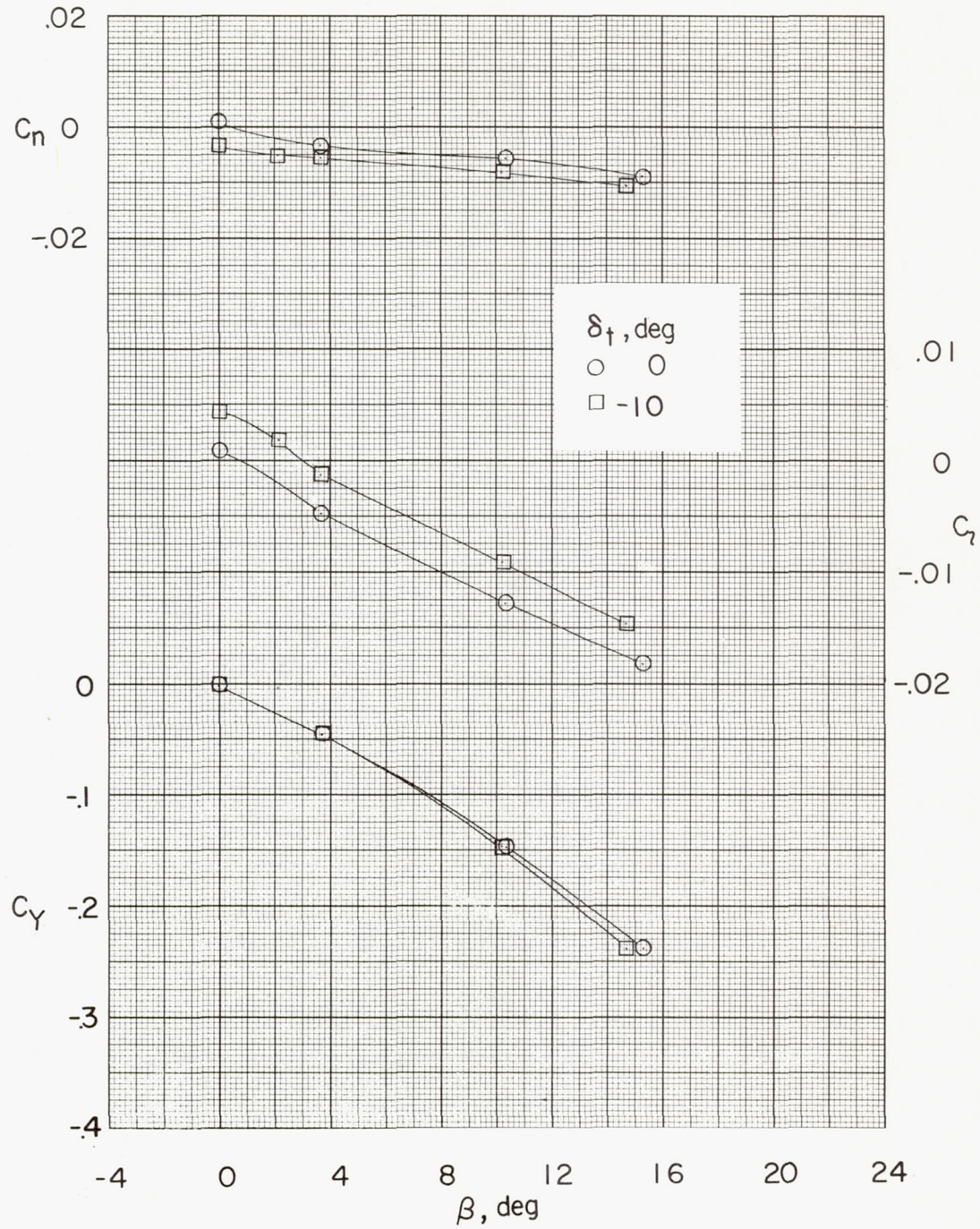
(c) $\alpha \approx 8.5°$.

Figure 3.- Continued.



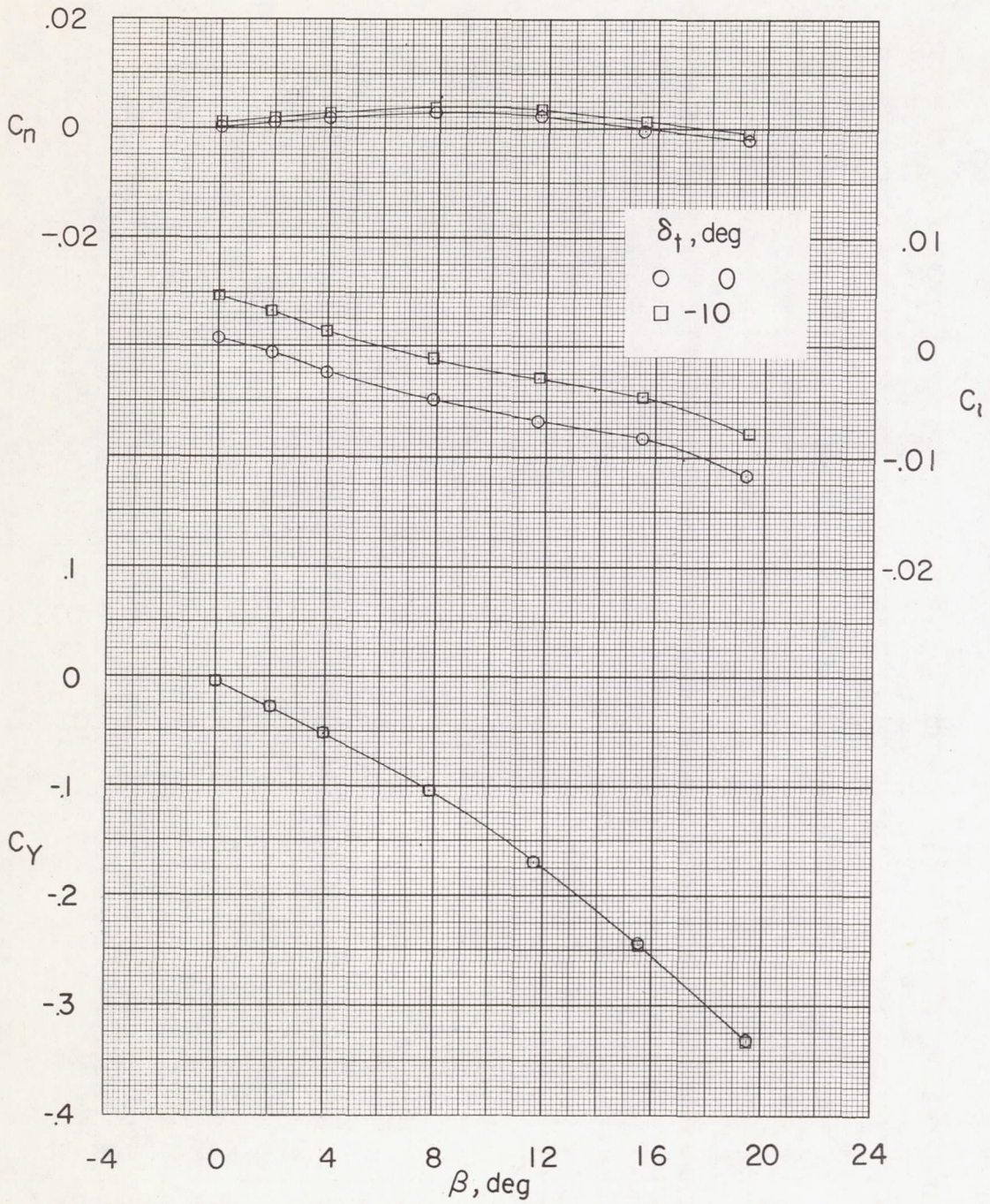
(d) $\alpha \approx 12.7^{\circ}$.

Figure 3.- Continued.



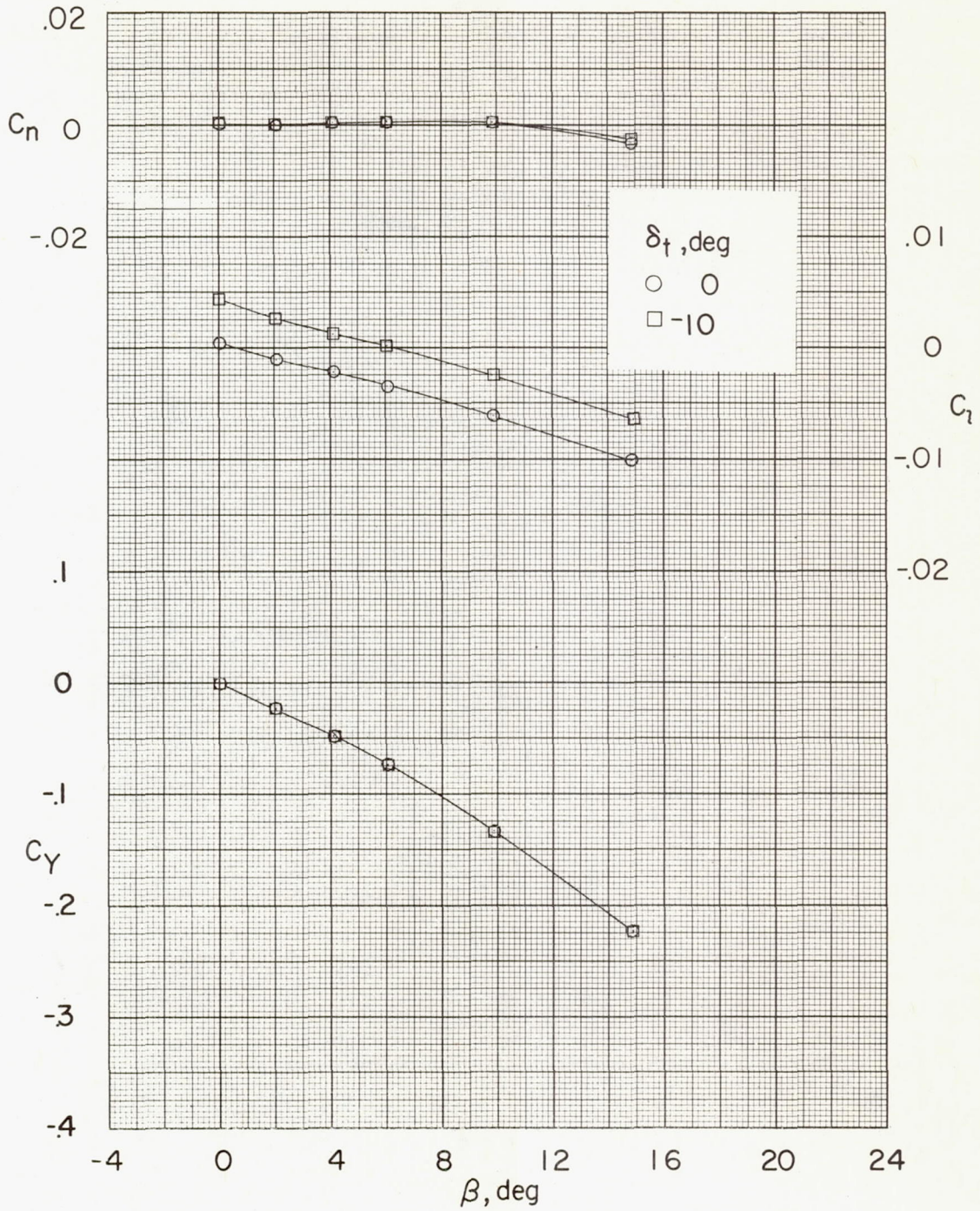
(e) $\alpha \approx 16^\circ$.

Figure 3.- Concluded.



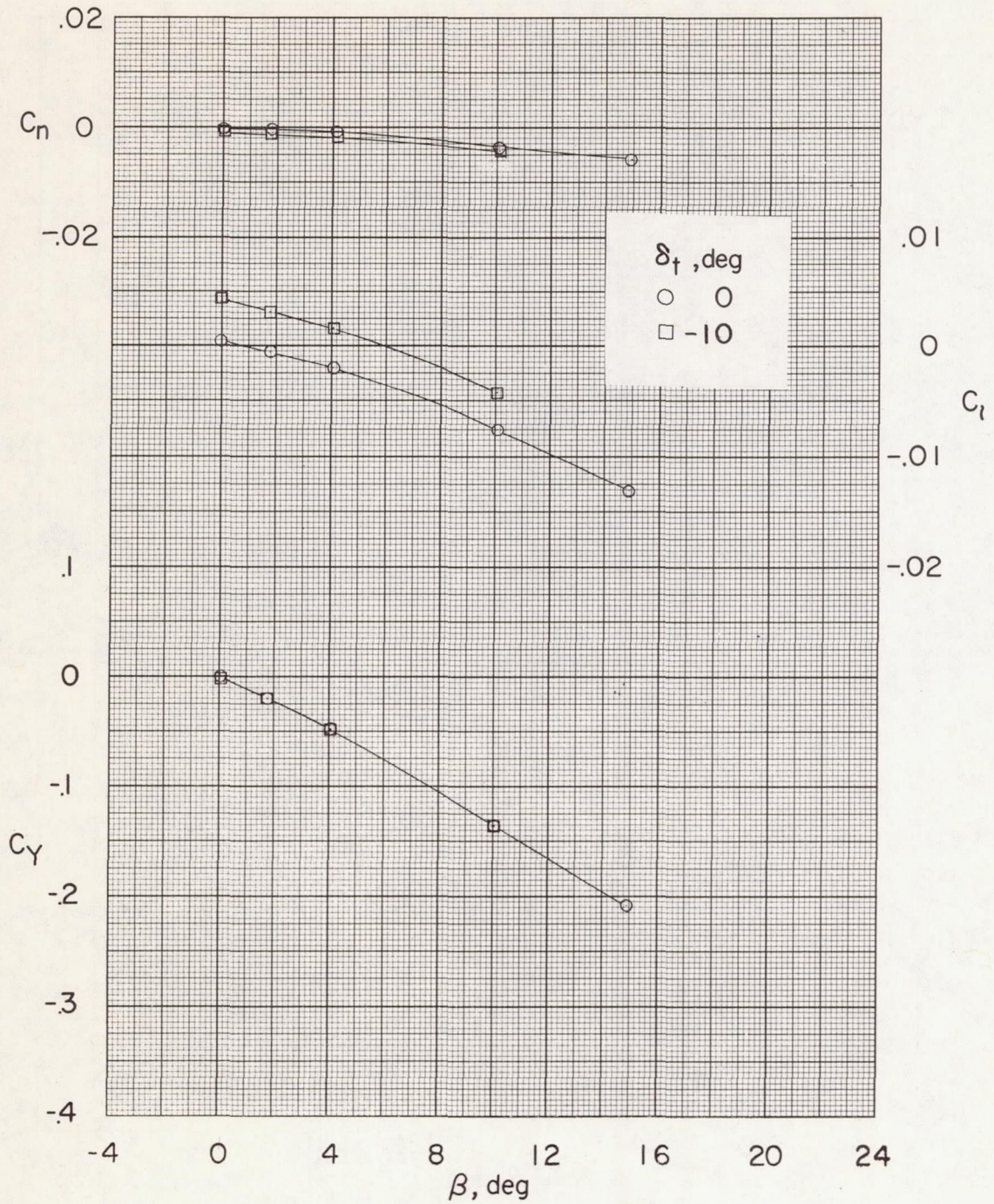
(a) $\alpha \approx 0^\circ$.

Figure 4.- Effect of differential stabilizer deflection on the aerodynamic characteristics in sideslip. Model 1; M = 2.01.



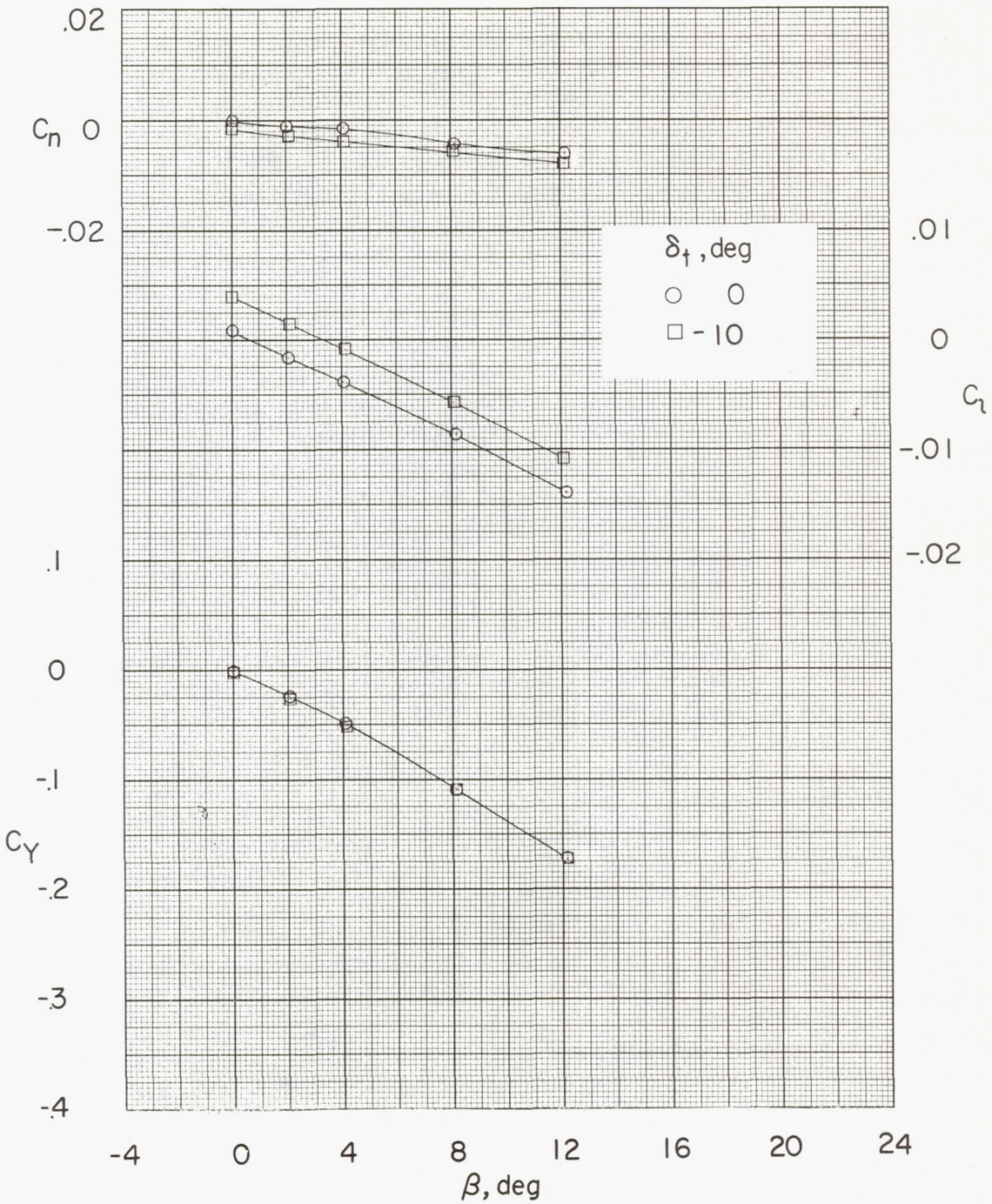
(b) $\alpha \approx 4.1^{\circ}$.

Figure 4.- Continued.



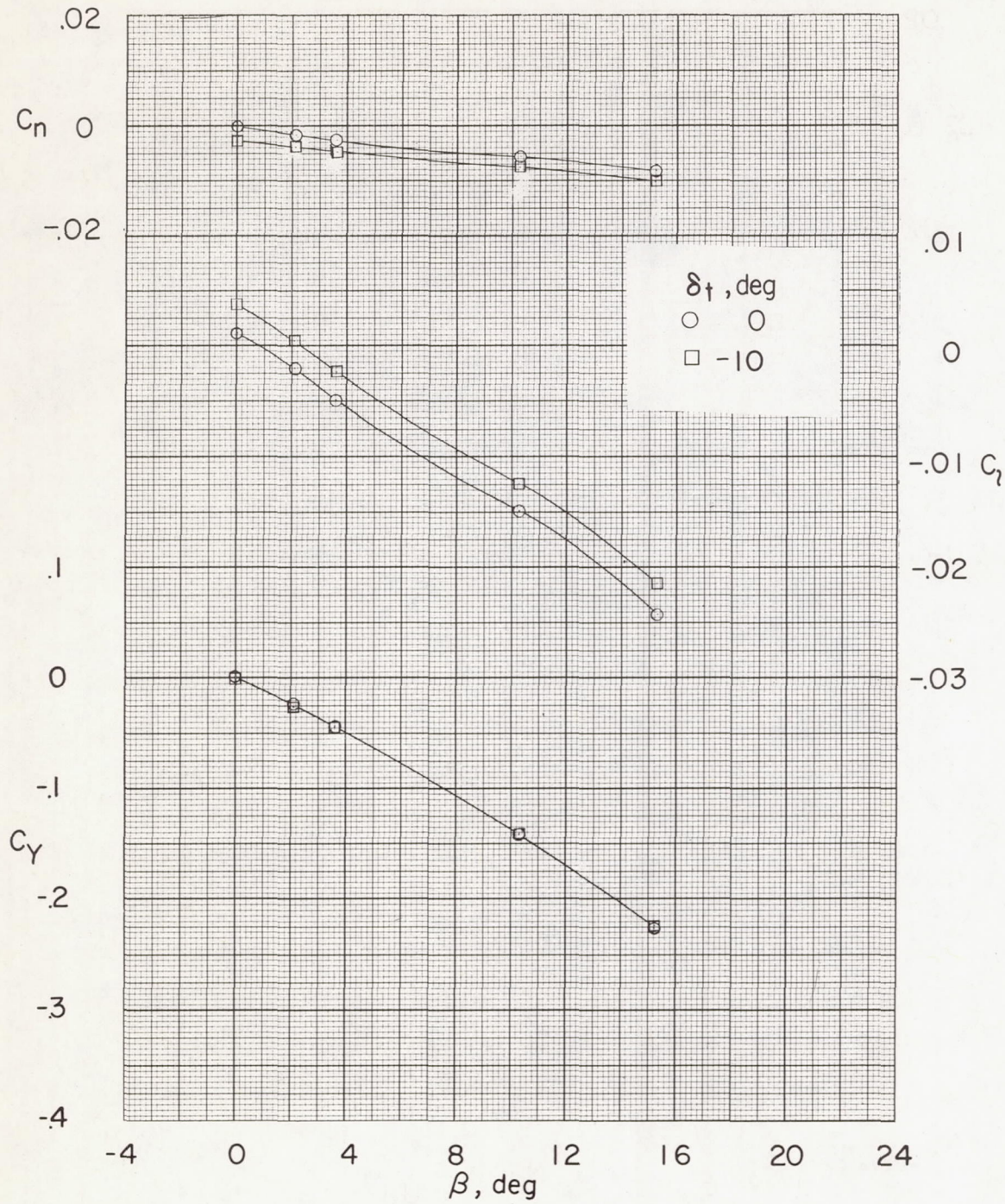
(c) $\alpha \approx 8.3^\circ$.

Figure 4.- Continued.



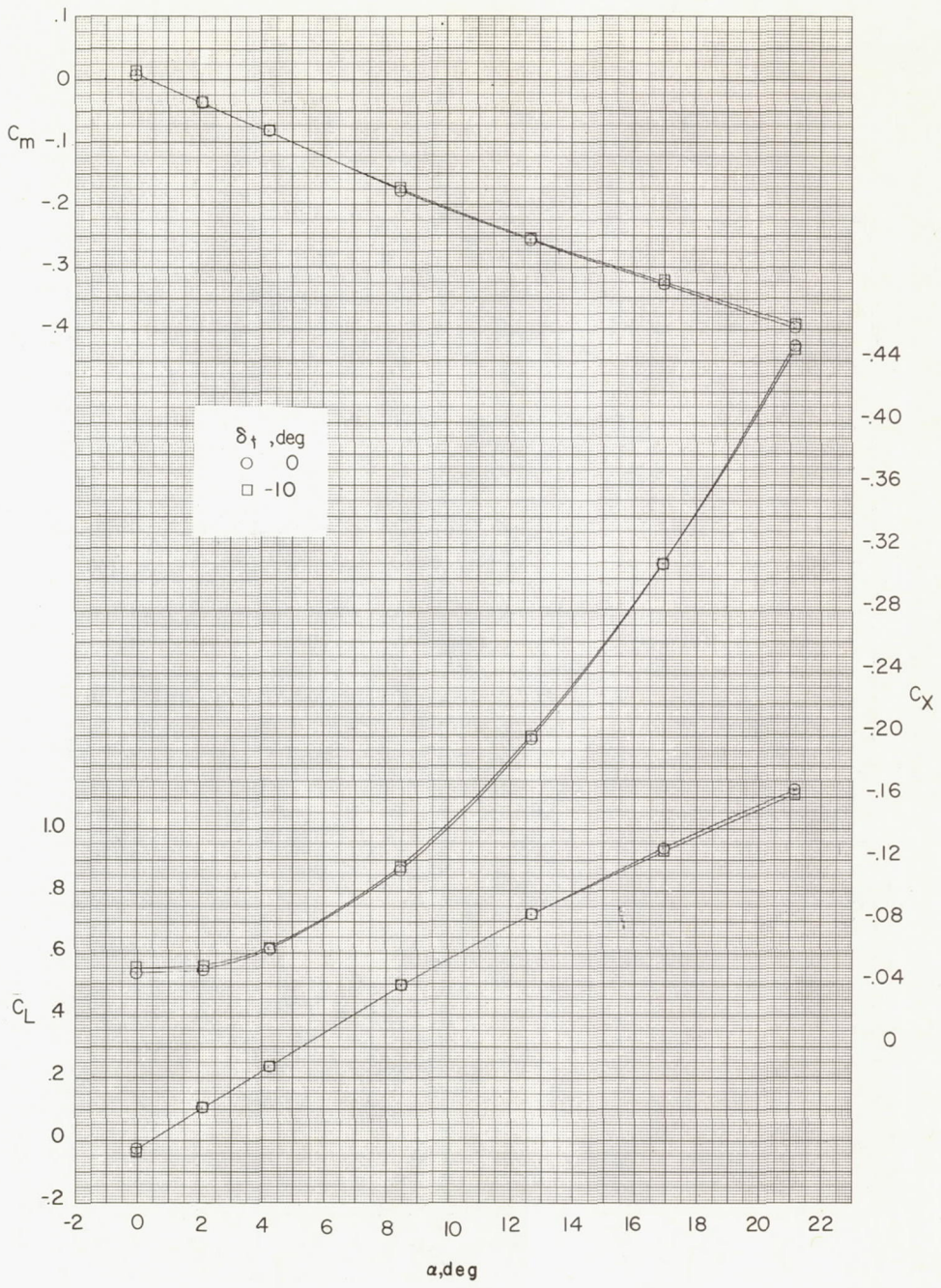
(d) $\alpha \approx 12.5^{\circ}$.

Figure 4.- Continued.



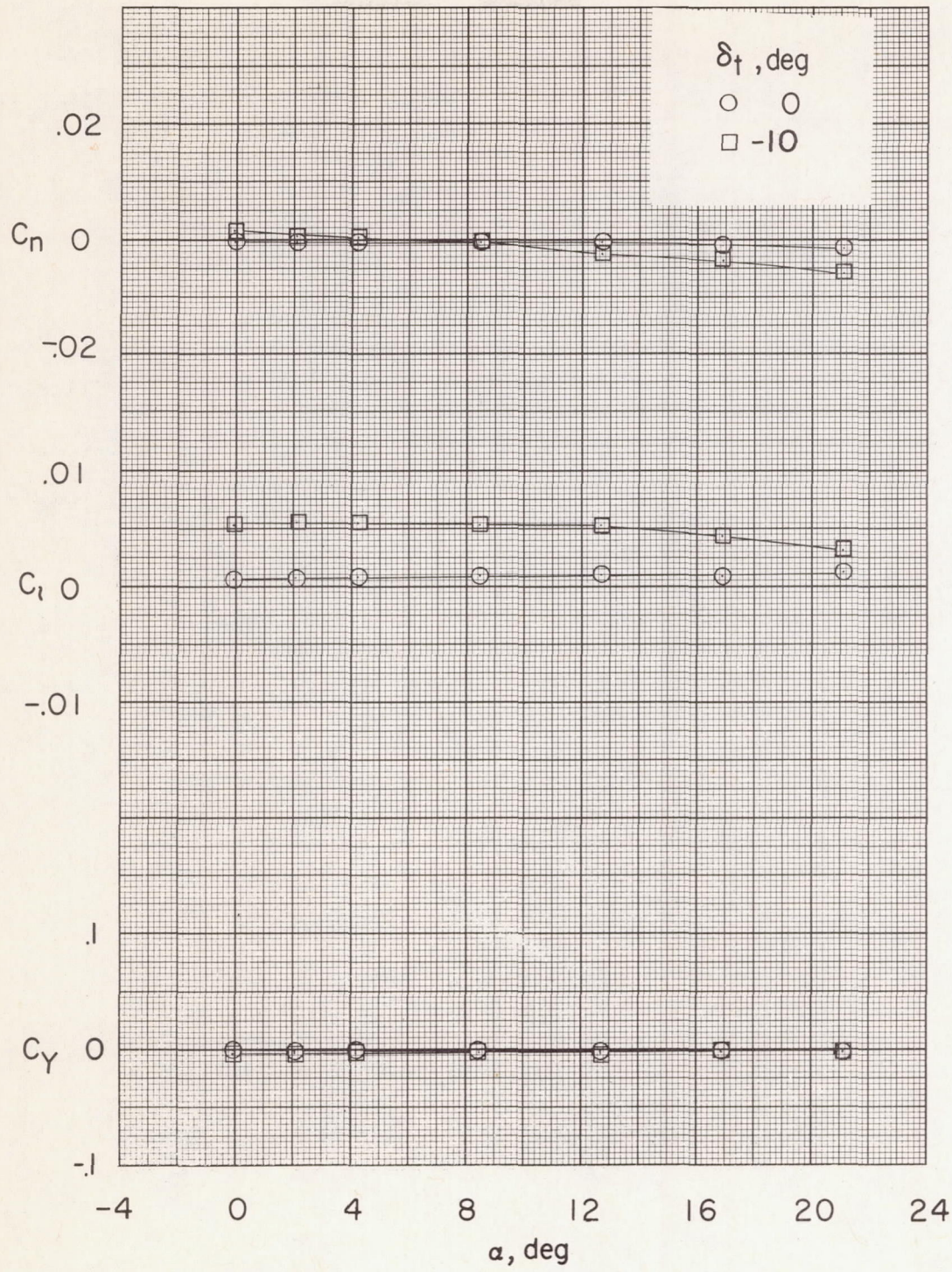
(e) $\alpha \approx 15.5^\circ$.

Figure 4.- Concluded.



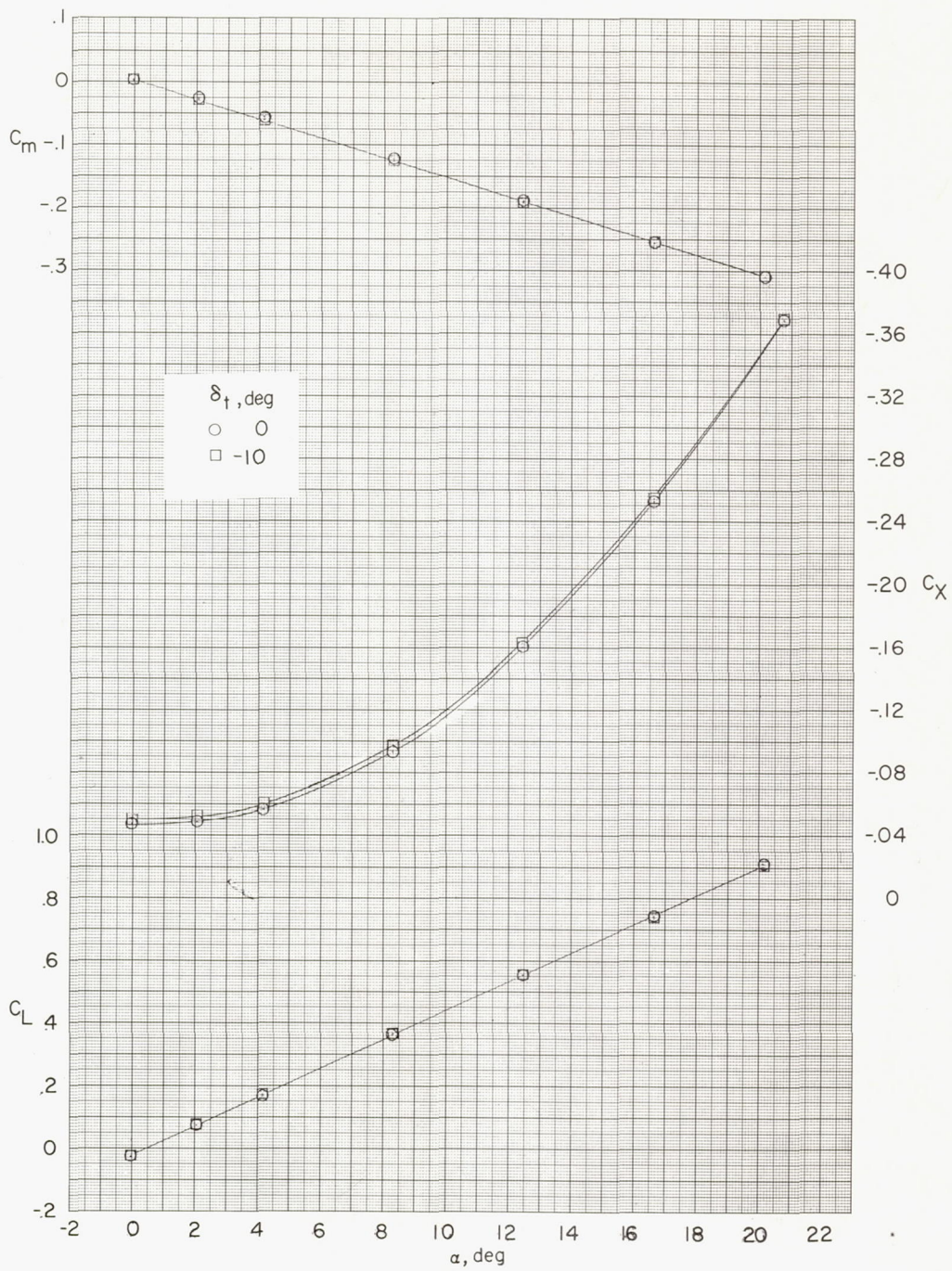
(a) C_m, C_L, and C_X plotted against α.

Figure 5.- Effect of differential stabilizer deflection on the aerodynamic characteristics in pitch. Model 1; M = 1.61; $\beta = 0^\circ$.



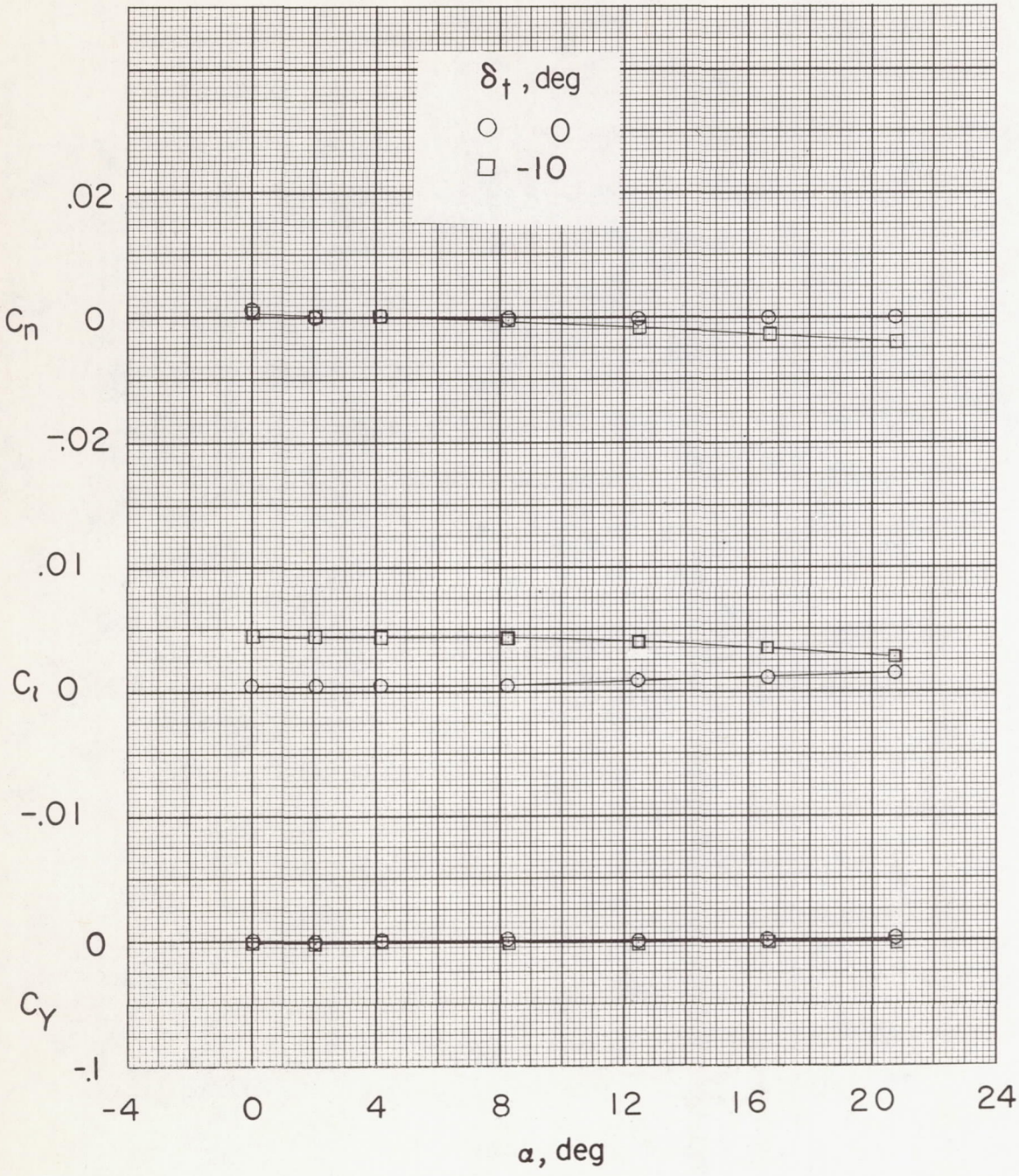
(b) C_n, C_l, and C_Y plotted against α.

Figure 5.- Concluded.



(a) C_m, C_X, and C_L plotted against α.

Figure 6.- Effect of differential stabilizer deflection on the aerodynamic characteristics in pitch. Model 1; M = 2.01; $\beta = 0^\circ$.



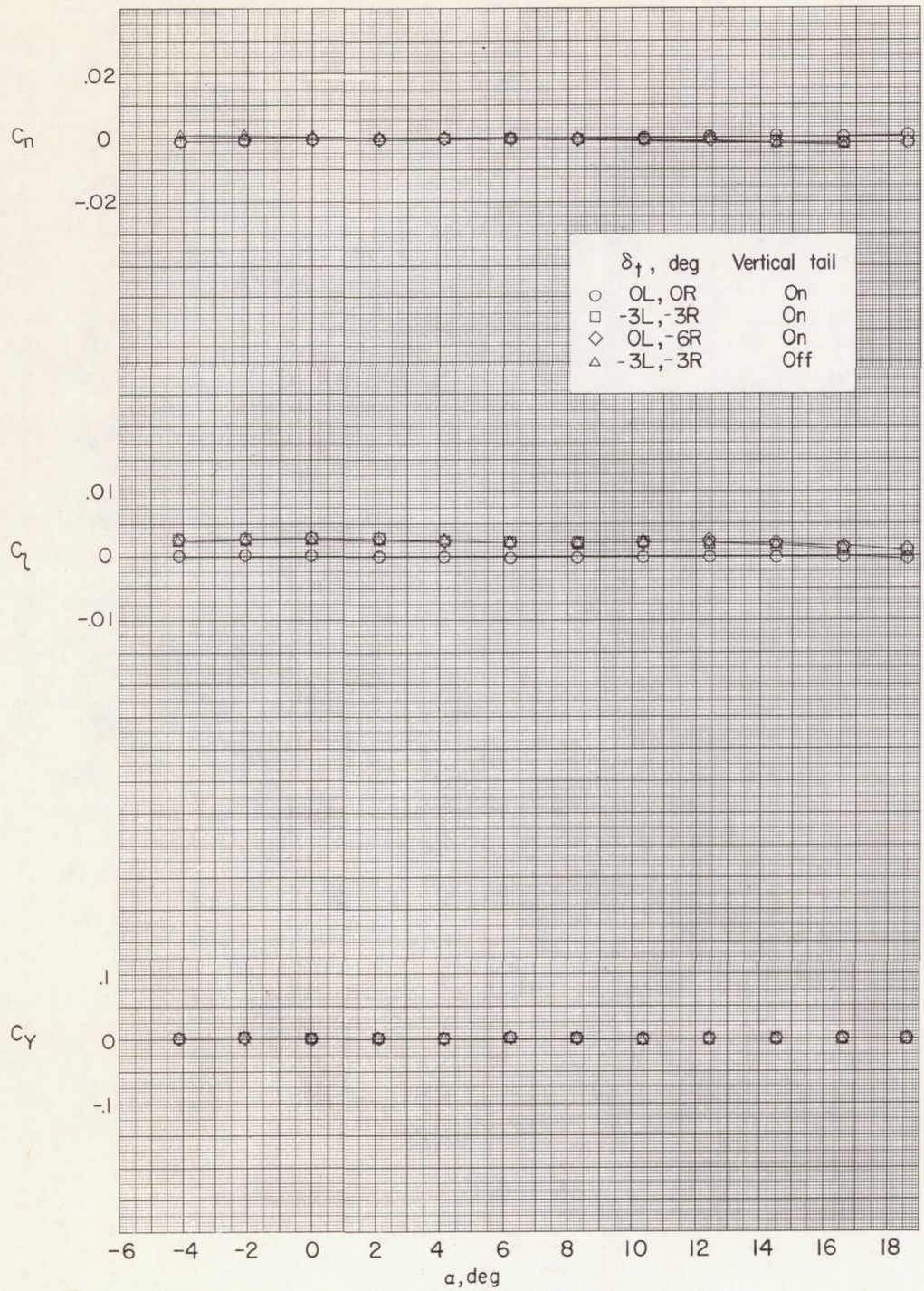
(b) C_n, C_l, and C_Y plotted against α.

Figure 6.- Concluded.



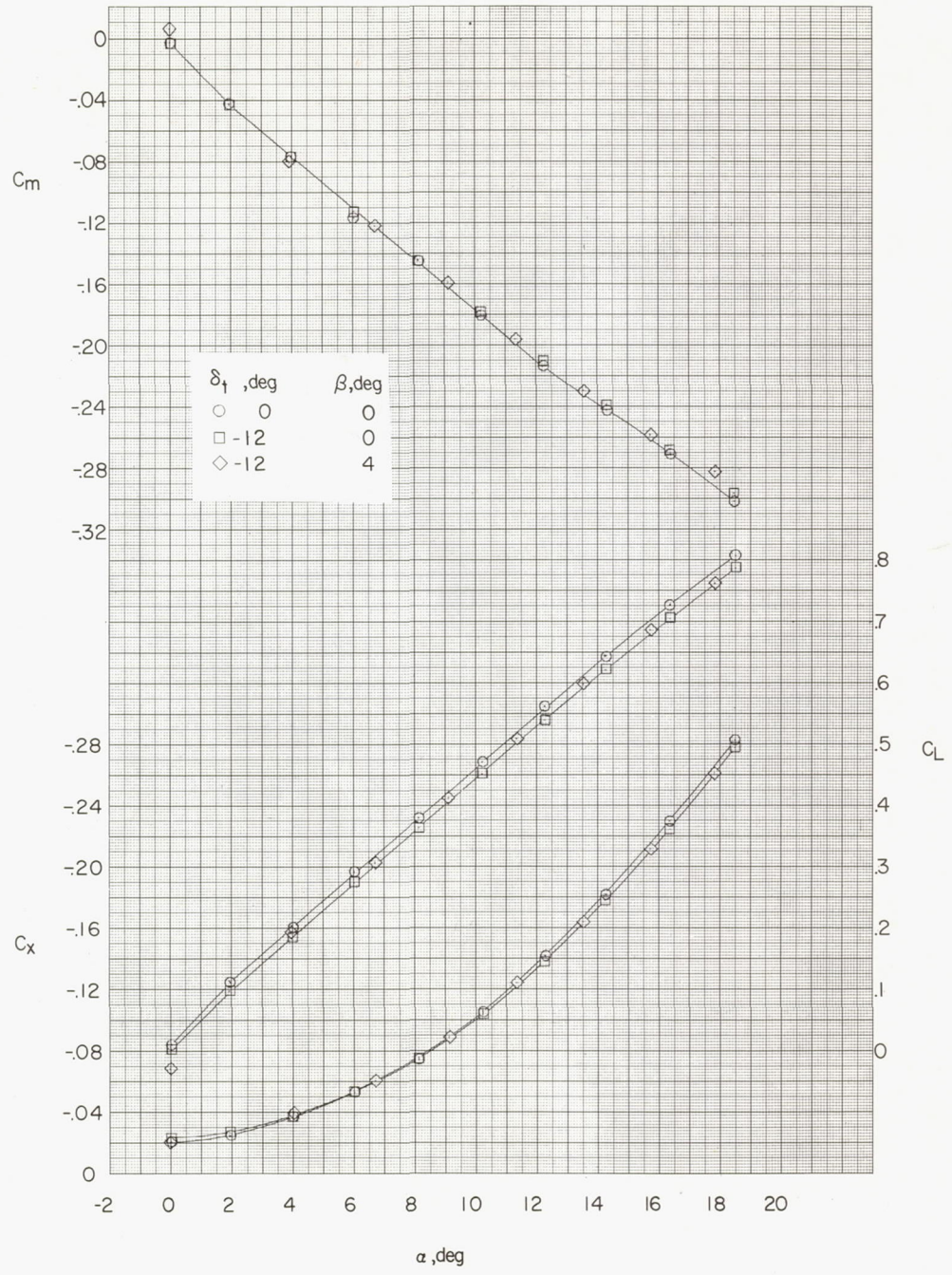
(a) C_m, C_L, and C_X plotted against α.

Figure 7.- Effect of differential stabilizer deflection on the aerodynamic characteristics in pitch. Model 2; M = 1.41; β = 0°.



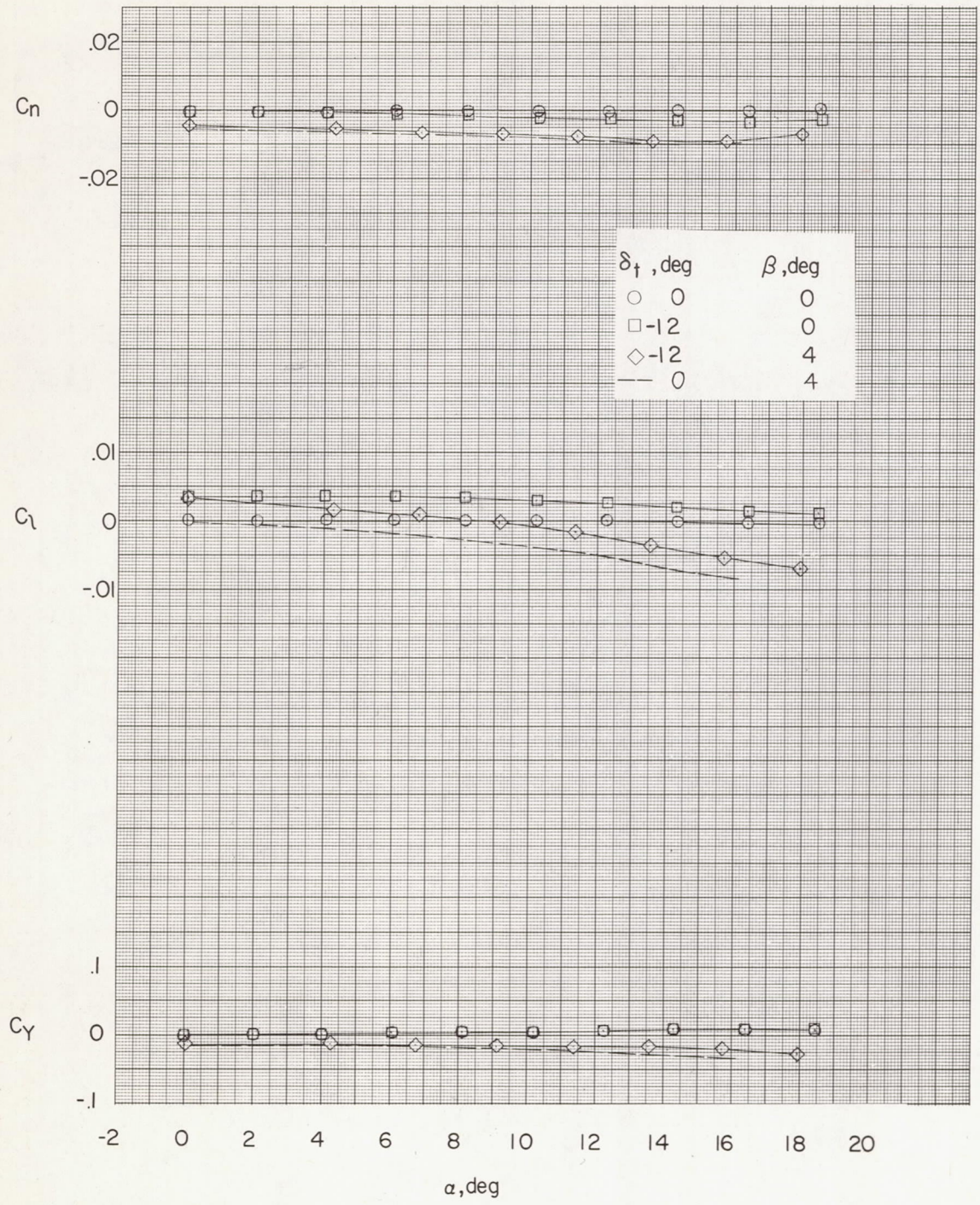
(b) C_n, C_l, and C_Y plotted against α.

Figure 7.- Concluded.



(a) C_m, C_L, and C_X plotted against α.

Figure 8.- Effect of differential stabilizer deflection on the aerodynamic characteristics in pitch. Model 2 with vertical tail removed; M = 2.01; $\beta = 0^\circ$ and 4°.



(b) C_n, C_l, and C_Y plotted against α.

Figure 8.- Concluded.

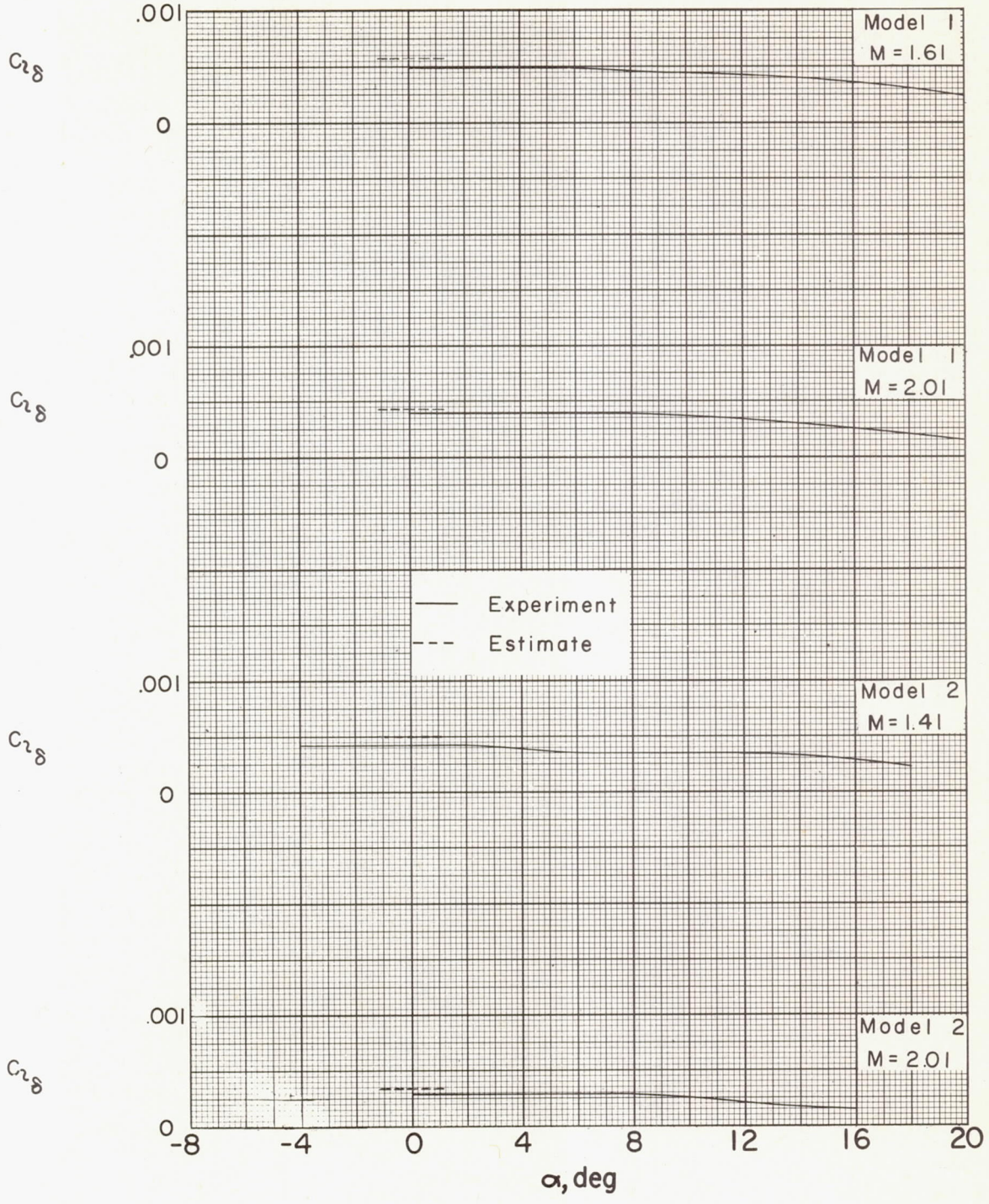


Figure 9.- Variation of roll-effectiveness parameter with angle of attack.

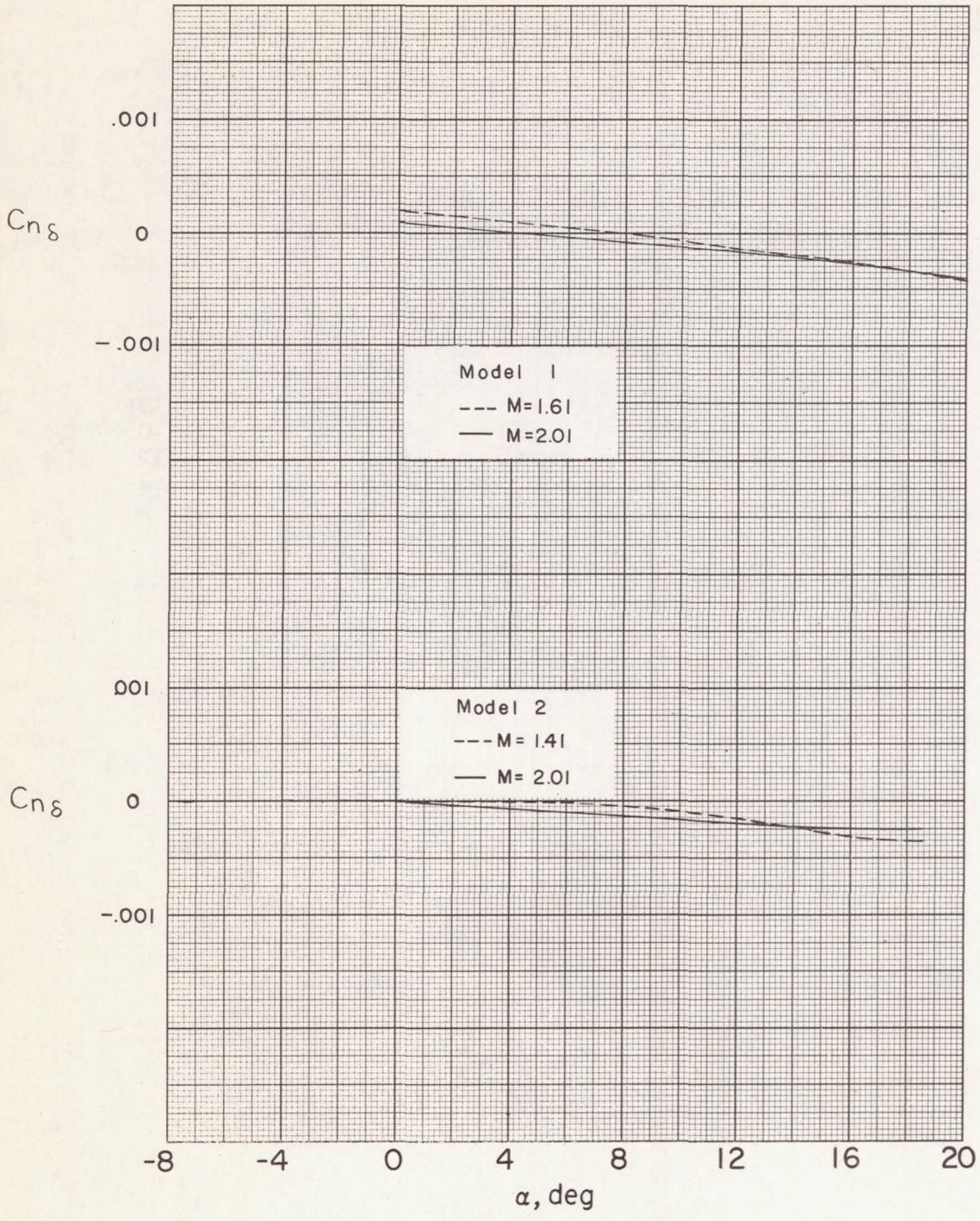


Figure 10.- Variation of yawing moment due to control deflection with angle of attack.

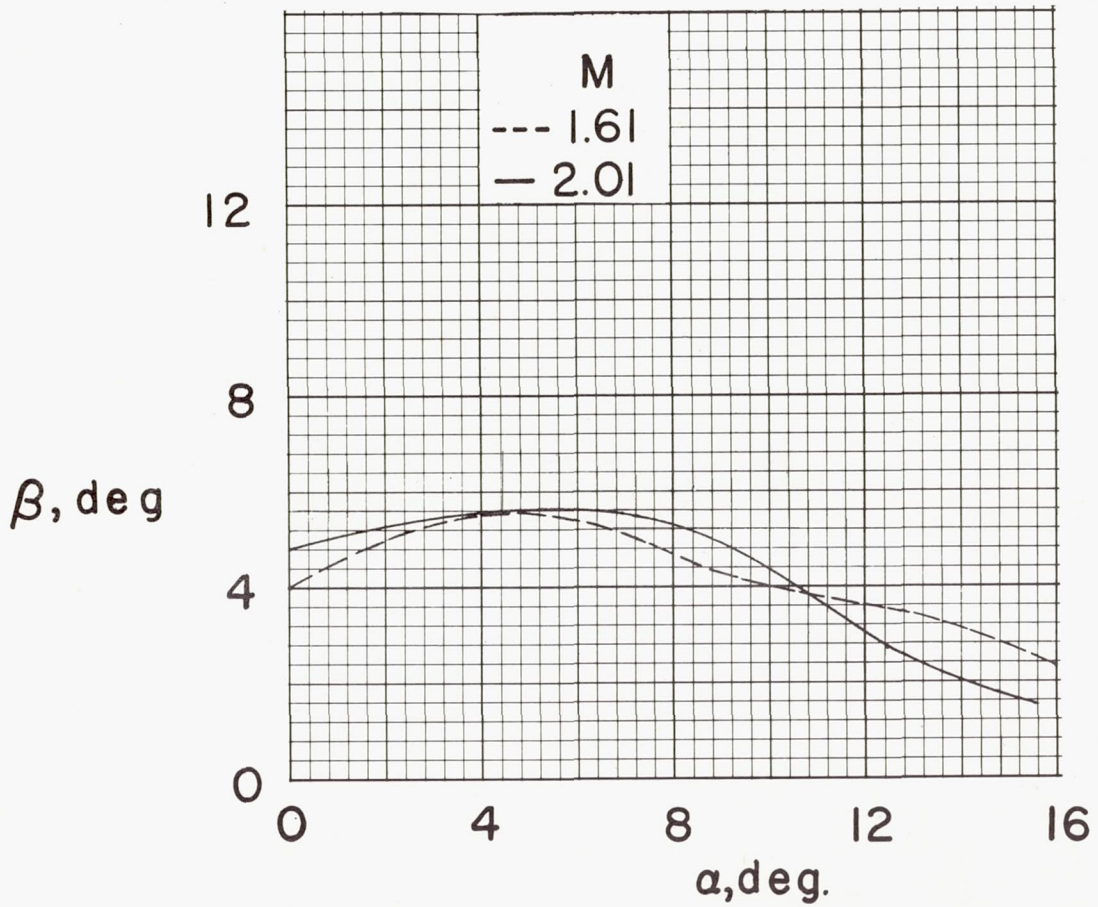


Figure 11.- Variation of sideslip angle for trim roll with angle of attack for $\delta_t = -10^\circ$. Model 1.